RSC Advances

PAPER

View Article Online
View Journal | View Issue

Cite this: *RSC Adv.*, 2023, **13**, 11044

Microwave assisted synthesis of fluorescent hetero atom doped carbon dots for determination of betrixaban with greenness evaluation†

Mariam S. El-Semary,[a] Ali A. El-Emam,[a] F. Belal[b] and Amal A. El-Masry *[a]

A simple, rapid and eco-friendly method for synthesis of nitrogen and sulfur doped carbon dots (N,S-CDs) is described. The method involved one step carbonization assisted by a green microwave irradiation route using available and cheap sources, as sucrose (source for C) and thiourea (source for N and S). The formed aqueous solution of N,S-CDs showed excellent optical and electronic properties with high compatibility and stability. The particles of the prepared dots were spherical with a narrow range of size from 1.7 to 3.7 nm with a quantum yield of 0.20. These dots act as a fluorescent probe, as they showed an intense blue fluorescence at 413 nm after excitation at 330 nm. The N,S-CDs were utilized for determination of the anticoagulant drug, betrixaban maleate (BTM), based on quenching of their fluorescence upon its gradual addition. The quenching process was found to be through an inner filter effect mechanism. The proposed method showed a good linearity over a concentration range of (1.0–100.0 μM) with LOD and LOQ values of 0.33 μM and 0.99 μM, respectively. All validation parameters met the acceptance criteria according to ICH guidelines. The high specificity and sensitivity of the performed method contributed to further assay of BTM in dosage form and spiked human plasma sample with high percent recoveries and low values of RSD. Interference from co-administered drugs was studied. Finally, the greenness of the proposed method was evaluated adopting a ComplexGapi approach, the excellent green profile has supported its applicability in quality control laboratories.

Received 7th February 2023
Accepted 30th March 2023

DOI: 10.1039/d3ra00824j

rsc.li/rsc-advances

Introduction

The significant value of anticoagulant drugs for treating many diseases, especially the century's disease "Covid-19", encouraged us to investigate the newly approved FDA anti-coagulant drug (Betrixaban maleate; BTM), which is one of the most recent direct oral Xa factor inhibitors.[1] It is considered as a more preferable alternative in treatment of stroke and venous thromboembolism when compared with vitamin K antagonist anticoagulants such as Warfarin, as it doesn't cause serious drug interactions or bleeding problems. BTM has a unique pharmacokinetic profile, as it has a rapid onset of action after oral administration with a long half-life of about 19 hours.[2] BTM is characterized by low possibilities in producing adverse drug effects and undesirable interaction with co-administered drugs or co-ingested food. Unlike other direct oral Xa factor inhibitor drugs, BTM does not induce or inhibit cytochrome P450 activity and is barely metabolized (<1%) by cytochrome enzymes. However, adjustment of BTM doses must be under consideration when being co-administered with P-glycoprotein inducers or inhibitors to avoid low pharmacodynamics of BTM or excessive effects. Furthermore, concomitant administration of other antiplatelets or thrombolytic drugs with BTM must be avoided due to the probability of increased bleeding. The oral bioavailability of BTM is also influenced by fatty foods, as the peak concentration of BTM is reduced by fifty percent when concomitantly taken with fatty meals.[2] The IUPAC name of BTM is: *N*-(5-chloropyridin-2-yl)-2-(4-(*N*,*N*-dimethylcarbamimidoyl) benzamido)-5-methoxybenzamide.[3] 2D and 3D manifestation of BTM structure was added in (Fig. 1). There are few reported methods for its quantification such as RP-HPLC,[4,5] LC/MS-MS,[6] spectrophotometry[7] and quantitative proton nuclear magnetic resonance.[8] The eagerness of the present work is that no spectrofluorometric methods have been yet reported for its determination. Herein, it will be an opportunity to develop a unique, sensitive, eco-friendly and fast quantitative method for determination of BTM in bulk, pharmaceutical preparations and biological fluids (spiked human plasma).

Recently, nano-sensing technology has become substantially involved in electrochemical detection strategies. Carbon-based dots are a central topic in nanotechnology, they are semiconductor nanocrystals with ultimately small size (below 10 nm).

[a]*Department of Medicinal Chemistry, Faculty of Pharmacy, Mansoura University, 35516 Mansoura, Egypt. E-mail: dr.Amal90@mans.edu.eg; Fax: +20 502200242; Tel: +20 502200520*

[b]*Department of Pharmaceutical Analytical Chemistry, Faculty of Pharmacy, Mansoura University, 35516 Mansoura, Egypt*

† Electronic supplementary information (ESI) available. See DOI: https://doi.org/10.1039/d3ra00824j

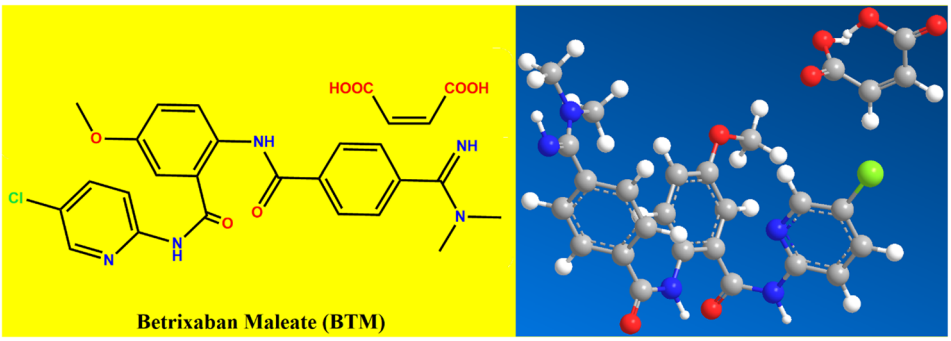

Fig. 1 2D and 3D manifestation of betrixaban maleate (BTM) structure.

These dots are characterized by high water solubility, minimal toxicity, good chemical stability and biocompatibility. They show distinctive electronic characters due to the high ratio between surface to volume. One of the manifest results from these characters is their bright fluorescence and reliable photoluminescence properties,[9,10] where different colors could be produced depending on the particle size. These dots could be prospective competitors or potential replacements for the fluorescent dyes or fluorescent complexing agents. Carbon dots could be categorized into different types such as graphene quantum dots (GQDs) and carbon quantum dots (CQDs) or heteroatoms-doped CQDs. The first one is considered as a graphene structure, which comprised of various layered sheets of sp^2 hybridized carbon with lateral dimensions lower than 10 nm.[11] In contrast, CQDs are similar to amorphous carbon which consist of a disordered sp^2 and sp^3 hybridized carbon structure with physical dimensions lower than 10 nm.[12]

There are different approaches that were currently demonstrated in the synthesis of nano sized carbon-based quantum dots, such as cleaving the large carbon structure as graphite and converting it into graphite oxide through multiple processing steps utilizing strong chemicals or laser ablation.[13] Carbonization or polymerization of organic precursors under different conditions such as hydrothermal, thermal or solvothermal is the simplest approach and is mostly utilized for synthesis of CQDs. This is due to its cost effectiveness, superior photo-

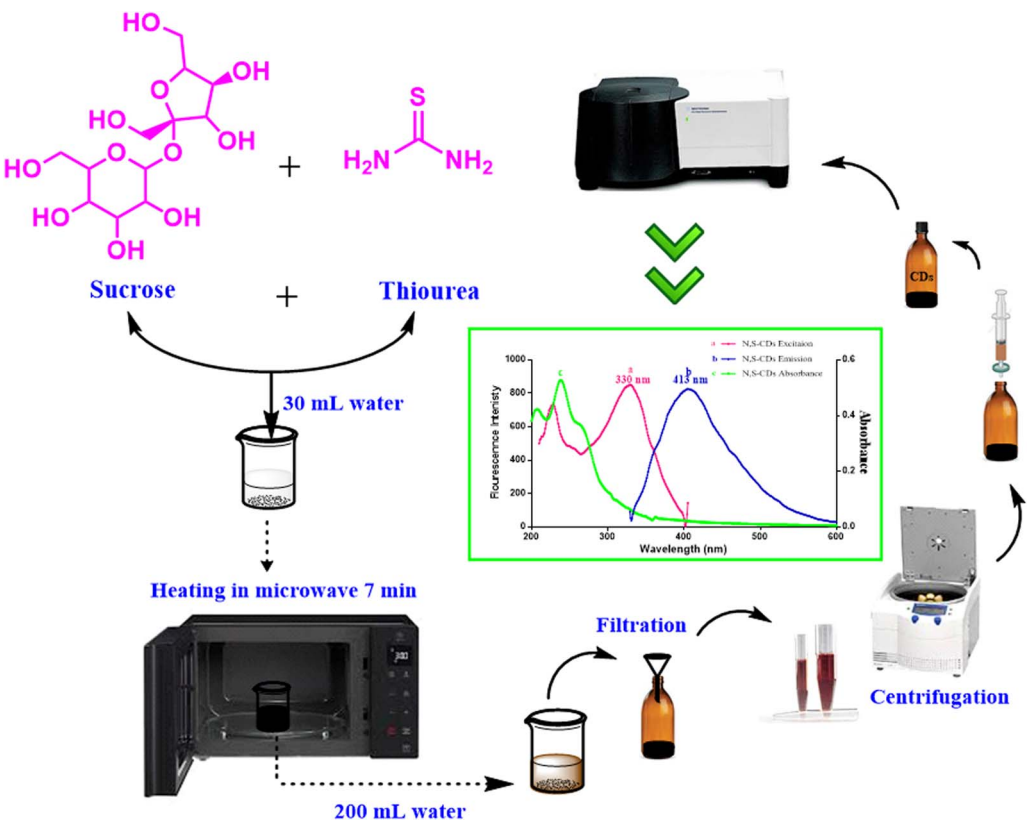

Fig. 2 Schematic sketch clarified the stepwise synthesis process of N,S-CDs.

physical properties, as well as high yield.[12] There are different applications which were inspired from the flexible synthesis of CQDs through different approaches and precursors. Some of these applications are photo-catalysis,[13,14] bio-imaging,[15] bio-sensing,[16] medical diagnosis,[17] and energy storage applications.[18–20] Outstanding features of CQDs with possible evolution of advanced technology and characterizations could extend the scope of CQDs applications and bring bright prospects.

The creativity in this study is based on synthesis of good optical and electronic properties with intense fluorescence N,S-doped CDs from cheap and eco-friendly precursors, such as sucrose and thiourea *via* green microwave irradiation route. The schematic sketch clarified the stepwise synthesis process of S,N-CDs was abridged in (Fig. 2). The main disadvantages of the previous reported methods concerning synthesis of quantum dots are high temperatures needed, long time consuming, and high electricity consumption.[21,22] All these defects were overcome by the utility of microwave, where the reaction was completed and the dots were formed within few minutes. Besides, the necessity of integrating green chemistry and achieving safety in the laboratory was embraced by applying a green strategy in synthesis of N,S-doped CDs. The synthesized hetero-atom CDs were used as fluorescent probe for quantitative determination of BTM in bulk, tablets and spiked human plasma, where BTM addition resulted in a decrease of the N,S-CDs fluorescence intensity in a quantitative manner.

Experimental

Instruments

Agilent Cary Eclipse Fluorescence Spectrophotometer was operated at high voltage (800 V) and fitted with Xenon flash lamp with slit width of 5 nm and high resolution. For spectrophotometric measurements, Shimadzu UV-1601PC UV/Visible double beam spectrophotometer was used. JEM-2100 transmission electron microscope (JEOL, Japan) was used for HR-TEM imaging. Oxford X-Max 20 silicon drift detector with scanning electron microscope (Jeol-jsm-6510 lv) was used for the energy dispersive X-ray (SEM-EDX) analysis. The X-ray diffraction (XRD) analysis for the crystallinity and phase purity of the CDs was performed using Bruker Co., Germany (D8 Discover XRD) with Cu Kα irradiation and wavelength of 1.54 Å at 40 kV and 40 mA. FTIR spectrum was obtained by Thermo-Fisher Scientific Nicolet iS20 FTIR spectrometer with a resolution of 4 cm^{-1} in the mid-infrared range (4000–400 cm^{-1}) and KBr disc system. Heating was achieved by LG microwave oven (model no. MS3043BARS operating at 700 W). pH Meter, Accu-lab (USA) pH-27B was utilized for adjustment the pH of the buffer solutions. Centrifugation was performed *via* Sigma 2-16P Benchtop Centrifuge.

Chemicals and materials

BTM (99.78% purity) was purchased from Portola Pharmaceutical Company, China. Lercanidipine hydrochloride (99.90% purity) was obtained from Recordati Industria Chimica E Farmaceutica S.P.A. (Italy). Rosuvastatin calcium (99.7% purity) was kindly provided by the Egyptian International Pharmaceutical Industry Co. (EPICO), Cairo, Egypt. Sodium hydroxide and boric acid were purchased from Piochem Co., Egypt. Glacial acetic acid 99%, orthophosphoric acid, sucrose, dextrose, lactose, sodium chloride and potassium chloride were acquired from EL-Nasr pharmaceutical company (ADWIC), Egypt. Ethanol (HPLC grade), quinine sulphate, ascorbic acid, thiourea, magnesium sulphate, ammonium chloride, sodium dihydrogen orthophosphate hydrate, zinc sulphate, oxalic acid, magnesium stearate and avisil were purchased from Sigma-Aldrich, Germany.

Human plasma was obtained from Mansoura University Hospital, Mansoura, Egypt and kept below −20 °C until used after thawing.

Preparation of nitrogen and sulfur doped carbon dots (N,S-CDs)

Synthesis of N,S-CDs was performed using domestic microwave-irradiation route with eco-friendly precursors such as sucrose (as carbon source) and thiourea (as nitrogen and sulphur source). They were prepared by dissolving 15 g of sucrose and 3 g of thiourea in 30 mL of distilled water then heating in microwave for 7 minutes until complete charring. The following sequential steps were followed in the same manner; the resulting N,S-CDs residue were left to cool, then mixed with 200 mL of distilled water, the obtained solution was filtered and centrifuged at 6000 rpm for 10 minutes. The supernatant was filtered through a 0.45 μm syringe filter and stored at room temperature protected from light. The working solution was freshly prepared by transferring 3.2 mL of stock solution into 100 mL volumetric flask, then it was completed to the mark with distilled water.

Estimation of quantum yield

Measuring the quantum yield of the synthesized N,S-CDs was performed using the following equation:[23]

$$\Phi_x = \Phi_{st} \times (F_x/F_{st}) \times (\eta_x/\eta_{st})^2 \times (A_{st}/A_x)$$

where: the symbols (Φ, F and A) are the quantum yield, the integrated intensity of emission and the absorbance, respectively. The symbol (η) is pointing to the solvent refractive index, where η_x/η_{st} in aqueous solutions is equivalent to 1. The subscript (x) refers to the unknown while (st) refers to the reference quinine sulfate sample. The reference quinine sulfate sample is prepared in 0.1 M sulfuric acid, where its quantum yield is 0.54 at 350 nm.[23]

Preparation of buffer solution

Britton Robinson buffer with pH range (2.5–12.2) was prepared by mixing equal molarities (0.04 M) of orthophosphoric acid, boric acid and acetic acid into 1 L volumetric flask, then adjusting the volume to the mark with distilled water. Different pH values of the buffer solution were obtained using different volumes of 0.2 M sodium hydroxide solution.[24]

Standard solutions

A weighed quantity (0.0284 g) of BTM was transferred into a 100 mL volumetric flask, dissolved in 30 mL of ethanol and the volume was completed to the mark with the same solvent to prepare a standard solution (500 μM). Further dilution of the stock solution was done as appropriate using ethanol. The standard solution was stored at −5 °C and remained stable for 7 days.

Construction of calibration curve

Different aliquots of the standard solution of BTM were transferred into a series of 10 mL volumetric flasks to obtain final concentrations of (1.0–100.0 μM), then mixed with 0.7 mL of working solution of N,S-CDs, followed by 2 mL aliquots of Britton Robinson buffer of pH 12. The solutions were then adjusted to the mark with distilled water. The relative fluorescence intensities (RFI) were determined for the reagent blank (F_0) and the drug (F) with N,S-CDs at 413 nm after excitation at 330 nm. The calibration graph is constructed by plotting $\ln(F_0/F)$ against final drug concentrations (μM). Calculations were done to derive the regression equation.

Determination of BTM in laboratory prepared capsules

Due to the unavailability of Bevyxxa Capsules in the Egyptian market, laboratory prepared capsules containing BTM and excipients, such as magnesium stearate, avisil, and dextrose were prepared to mimic the Bevyxxa dosage form. Ten capsules were weighed, evacuated completely, crunched, and merged for the assay of BTM content. A specific weight equivalent to 0.0284 g of BTM was transferred to 100 mL volumetric flask, mixed with ethanol to prepare final BTM stock solution with concentration of (500.0 μM). Thereafter, to guarantee perfect homogeneity and component solubility, this solution was sonicated for 10 minutes. Finally, the same procedure demonstrated under "Construction of Calibration Curve" was performed and the nominal contents of capsules were estimated from the regression equation.

Determination of BTM in human plasma

Into a series of 10 mL centrifuge tubes, 1 mL aliquots of plasma were added to each tube and then mixed with different concentrations of BTM to reach the final concentration in the range of (1.0–3.0 μM), sonicated for 10 seconds followed by the

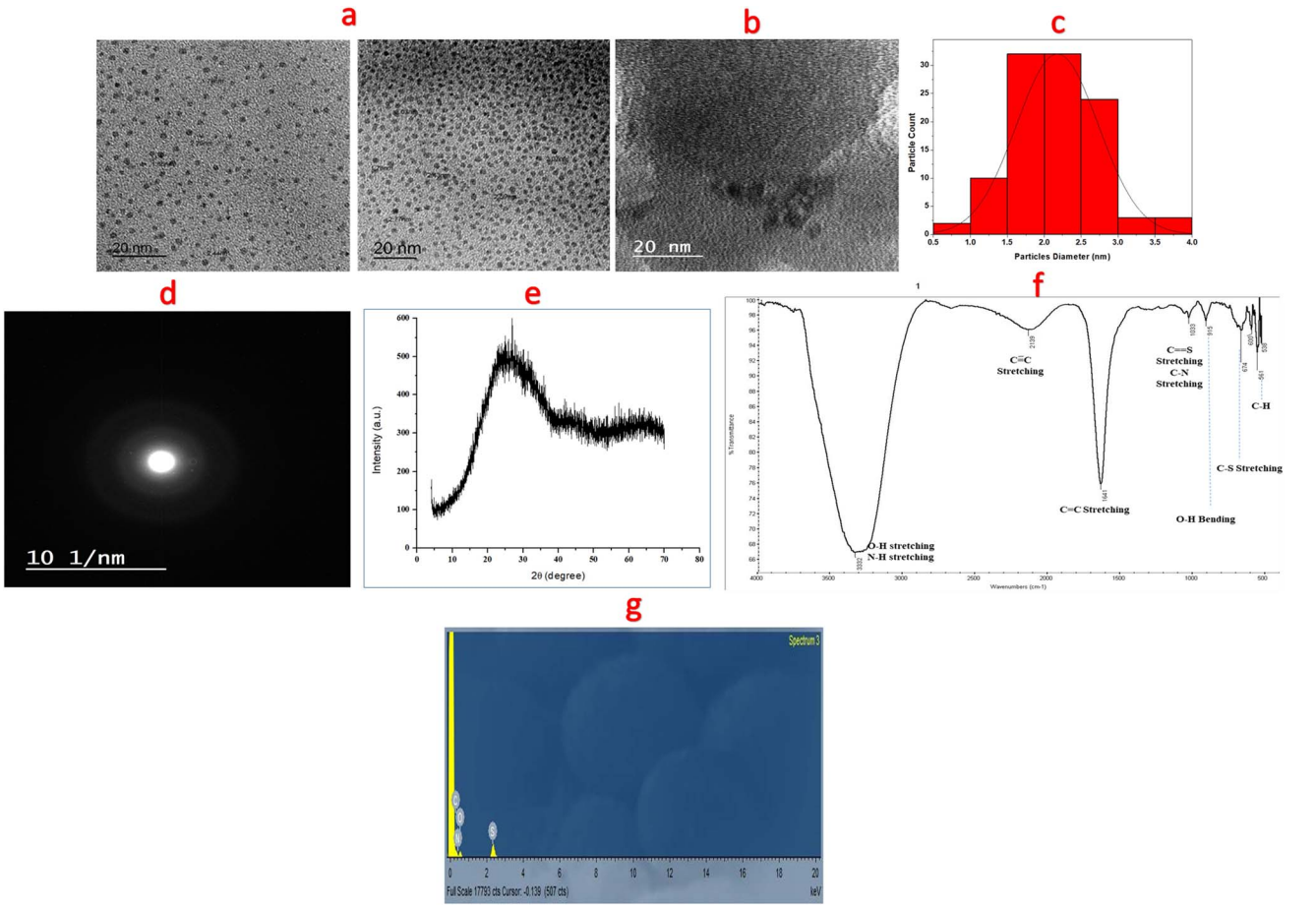

Fig. 3 The characterization of synthesized nanosensor (N,S-CDs) where, (a and b) are the remarkable spherical nano-particles showed *via* transmission electron microscopy and high resolution transmission electron microscopy, respectively, (c) is a particle size distribution histogram of a synthesized nanosensor, (d and e) are SAED and XRD patterns of the N,S-CDs, respectively. (f) Is the expected functional groups in the N,S-CDs illustrated by FT-IR spectra, while (g) is an energy dispersive X-ray spectrum of N,S-CDs.

addition of methanol up to 4 mL to precipitate the proteins. Subsequently, the mixture was sonicated for 10 seconds followed by centrifugation at 4500 rpm for 15 minutes, the supernatants were filtered through a 0.25 μm cellulose syringe filter. One mL aliquots of the clear filtrate were added into 10 mL volumetric flasks and the same procedure demonstrated under "Construction of Calibration Curve" was performed. Finally, the percent recoveries were estimated from the regression equation.

Results and discussion

Characterization of the synthesized dots

Different techniques were utilized for descriptive explanation of the synthesized dots. These dots (N,S-CDs) were simply prepared with high quantum yield (0.20) from sucrose and thiourea *via* microwave irradiation in a one-pot step as seen in (Fig. 2). The precise shape and size of the synthesized N,S-CDs were achieved by TEM. The results showed spherically and uniformly dispersed N,S-CDs particles with size range of 1.7–3.7 nm. The TEM image and a particle size distribution histogram were abridged in (Fig. 3a and c). Higher magnification of the observed HR-TEM image (Fig. 3b) with a good quality was difficult to be obtained as a result of low electron contrast between the N,S-CDs and the carbon coated copper grid. Nonetheless, the distinct dark dots visible in the HR-TEM image (Fig. 3b) are a sign that small, concentrated clusters of carbon atoms have been formed. The selected area electron diffraction (SAED) pattern displayed a diffused halo as appeared in (Fig. 3d) which indicates the amorphous nature of the prepared N,S-CDs. The typical amorphous nature of N,S-CDs was furthermore ensured by XRD pattern (Fig. 3e). The XRD pattern for the N,S-CDs showed a broad peak at $2\theta = 26.9°$, which is slightly shifted corresponding to the 002 plane of the graphite ($2\theta = 26.4°$). The interlayer spacing (d) of the N,S-CDs is 0.331 nm. Based on these consistent results, we can conclude that the prepared N,S-CDs are amorphous in nature.[25] FT-IR Spectroscopy was performed for determination of the surface functional groups of N,S-CDs. As apparent in FT-IR spectra (Fig. 3f), the broad band at 3332 cm^{-1} is corresponding to NH/OH groups. While, the absorption bands at 1641 cm^{-1} and 1033 cm^{-1} are corresponding to stretching vibration of C=C group and C=S group, respectively.[26] The narrow bands at 674 cm^{-1} and 561 cm^{-1} correspond to C–S group and C–H group, respectively. These findings proved the existence of oxygen, nitrogen and sulfur functional groups at the surface of the CDs and resulted in

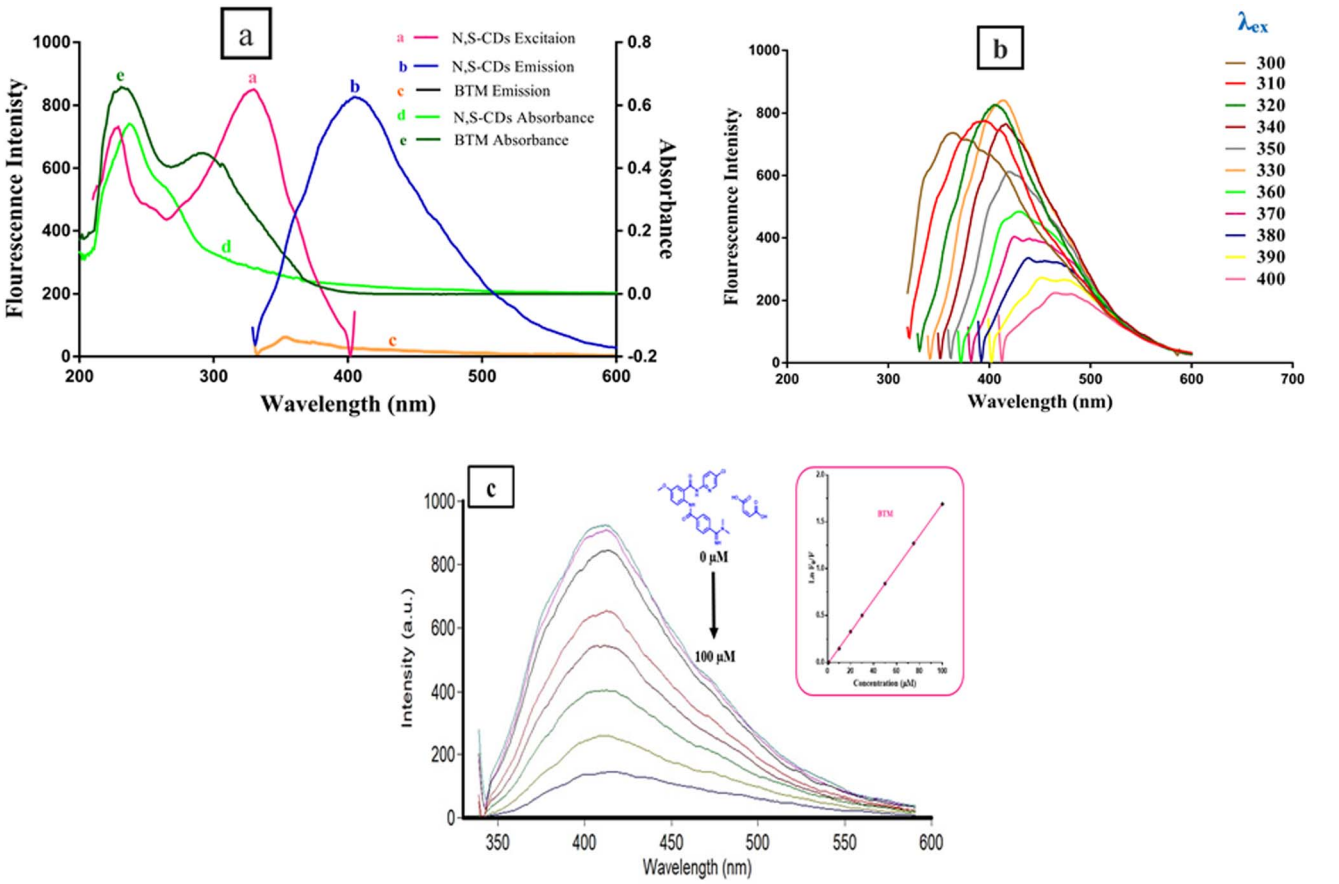

Fig. 4 (a) Excitation and emission spectra of N,S-CDs, emission spectrum of BTM alone as a control experiment, with UV-visible spectra of N,S-CDs and BTM. (b) Emission spectra of N,S-CDs after excitation at different wavelengths from 300 nm to 400 nm. (c) Quenching of the fluorescence emission of the N,S-CDs in quantitative manner upon adding an increasing concentrations of BTM (from blue to violet 0.0, 1.0, 10.0, 20.0, 30.0, 40.0, 50.0, 75.0, 100.0 μM).

greater improvement in its fluorescence and electronic behavior.[10,27] The energy dispersive X-ray spectroscopy (EDX) was performed to analyze the surface and elemental composition of the prepared N,S-CDs. The EDX results confirmed the presence of carbon (32.56%), nitrogen (36.68%), oxygen (28.93%) and sulfur (1.83%) as shown in an energy dispersive X-ray spectrum of N,S-CDs (Fig. 3g). UV-Vis absorption spectrum exhibited two peaks at 238 nm and 264 nm which are attributed to the trapped excited state energy by the surface state and n–π* transition of C–O and C–N groups causing strong emission.[21,28] The excitation and emission spectra of N,S-CDs, emission spectrum of BTM alone as a control experiment, and UV-visible spectra of N,S-CDs and BTM were drawn in (Fig. 4a). The aqueous solution of N,S-CDs possessed excitation wavelength dependent behavior, as upon increasing the excitation wavelength 10 nm in each (from $\lambda_{ex} = 300$ nm till $\lambda_{ex} = 400$ nm), results in changing their fluorescence and emission wavelengths. The highest intense blue fluorescence of these dots was achieved at $\lambda_{em} = 413$ nm *via* excitation at wavelength of 330 nm. The emission spectra of N,S-CDs after excitation at different wavelengths from 300 nm to 400 nm was abridged in (Fig. 4b). Doping nitrogen or sulfur atoms into the CDs leads to enhance the optical and electrical properties. Therefore, doping sulfur atom could provide the density of states or emissive trap states for photo-excited electron capture, which modifies the band-gap energy. It further avoids self-quenching due to its large ensemble stokes shift. Furthermore, doping nitrogen atom is of great importance in fabricating modified CDs. It has a comparable atomic size and five valence electrons that can fit well at the lattice position of carbon-based materials. It could inject electrons into CDs and change the internal electronic environment, which consequently improves fluorescence properties.[11,29]

Mechanism of fluorescent N,S-CDs quenching in response to BTM

The design of quantification of BTM in this study depends on turning off the fluorescence that results from the synthesized N,S-CDs ($\lambda_{ex} = 330$, $\lambda_{em} = 413$). The quenching was observed in a quantitative manner *via* increasing the concentration of BTM ranging from (1.0–100 μM) as shown in (Fig. 4c). There are different mechanisms that contribute to quenching the fluorescence of these dots by different analytes, such as inner filter effect (IFE), static quenching, dynamic quenching and fluorescence resonance energy transfer.[30] To understand the actual mechanism occurred with BTM, further investigation was performed. The UV-Vis spectrum of BTM showed an absorption peak at 307 nm which was overlapped with the excitation spectrum of N,S-CDs at wavelength of 330 nm (Fig. 4a), thus there is a possibility of occurring IFE or FRET.[31] By applying the following eqn (i) for further elucidation of the mechanism:

$$F_{corr} = F_{obs} \times \text{antilog}\left[\frac{A_{ex} + A_{em}}{2}\right] \quad \text{(i)}$$

where, F_{corr} is the corrected fluorescence intensity upon removing IFE from F_{obs}.

F_{obs} is the observed fluorescence intensity.

The absorbance of BTM (the quencher) is denoted by (A) at the excitation (ex) and emission (em) wavelengths of the fluorescent N,S-CDs.

Then the suppressed efficiency (E%) was calculated for both corrected and observed fluorescence intensity of N,S-CDs in accordance to the provided eqn (ii):

$$E(\%) = \left[1 - \frac{F}{F_0}\right] \times 100 \quad \text{(ii)}$$

A relationship between E of the corrected and observed fluorescence intensities and BTM concentrations in (μM) was constructed in (Fig. 5a), indicating that IFE was the mechanism that highly contributed to the fluorescence quenching of N,S-CDs by increased concentrations of the quencher (BTM).

Further investigation was conducted for illustrating the possibility of another quenching mechanism based on Stern–Volmer eqn (iii) through measuring the fluorescence emission intensities in case of existence and absence of the quencher at three temperatures settings (313 K, 323 K and 333 K).

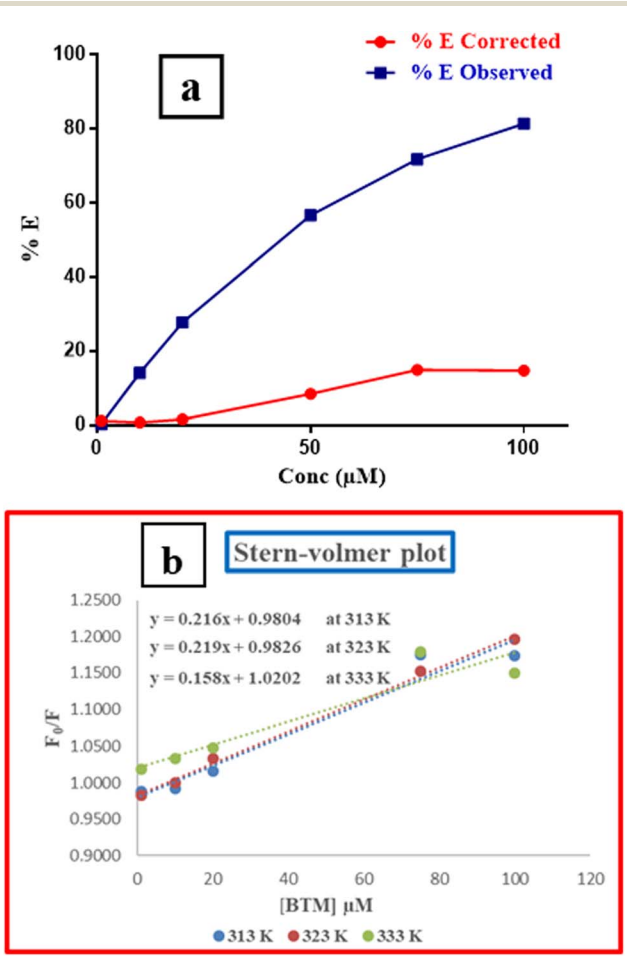

Fig. 5 (a) Percentage of suppressed efficiency of observed and corrected fluorescence of N,S-CDs after addition of various concentrations of BTM (μM). (b) The Stern–Volmer plot of (BTM-N,S-CDs) at different temperatures (Kelvin).

$$\frac{F_0}{F} = 1 + K_{sv}[Q] \quad \text{(iii)}$$

where, the fluorescence emission intensities are denoted by F_0 in the absence of BTM, while denoted by F in the existence of BTM.

K_{sv} is the symbol of the Stern–Volmer quenching constant, while [Q] is the symbol of the quencher (BTM) concentration.

By plotting a graph of F_0/F *vs.* molar concentrations of the quencher (Fig. 5b), it was found that, there was no effect on the quenching rate constant neither by increasing nor decreasing its value. Therefore, the possibility of quenching *via* dynamic or static mechanisms were excluded.

Stepwise-optimization of experimental features

pH of the buffer. The effect of changing pH on the fluorescence intensity of N,S-CDs was investigated over the pH range of (2.5–12.2) using Britton Robinson buffer as abridged in (Fig. 6a). Throughout the study, the highest F_0/F value was obtained by adjusting pH at 12.

Volume of the buffer solution. Different volumes of Britton Robinson buffer solution were tried in the range of 0.5–2.5 mL. The maximum quenching occurred upon the addition of 2 mL of the buffer (Fig. 6b).

Volume of N,S-CDs. Different volumes of N,S-CDs solution were tried in the range of 0.3–1 mL to reach the highest F_0/F value. Addition of 0.7 mL of N,S-CDs working solution gave the highest F_0/F value, so it was selected for the whole study (Fig. 6c).

Ionic strength. The influence of the addition of sodium chloride solution over the range of 0.1–2.0 M to the buffer solution was studied. The F_0/F value was found to remain constant which proved the steadiness of N,S-CDs against ionic activity (Fig. 6d).

Incubation time. The impact of incubation time was examined after the addition of BTM to N,S-CDs at different time intervals from 0.5 to 15 minutes. The quenching was found to be unaffected by the passage of time, and the reaction was completed within one minute and remained stable for more than half an hour.

Analytical performance. The validity of the proposed method was tested according to International Conference on Harmonization (ICH) guidelines.[32]

The method possessed good linearity upon plotting ln F_0/F over different BTM concentrations (μM) over a range of (1.0–100.0 μM).[31] High regression coefficient with low percentages of RSD and error were obtained as shown in (Table 1) upon statistical analysis of the output data with regression equation:

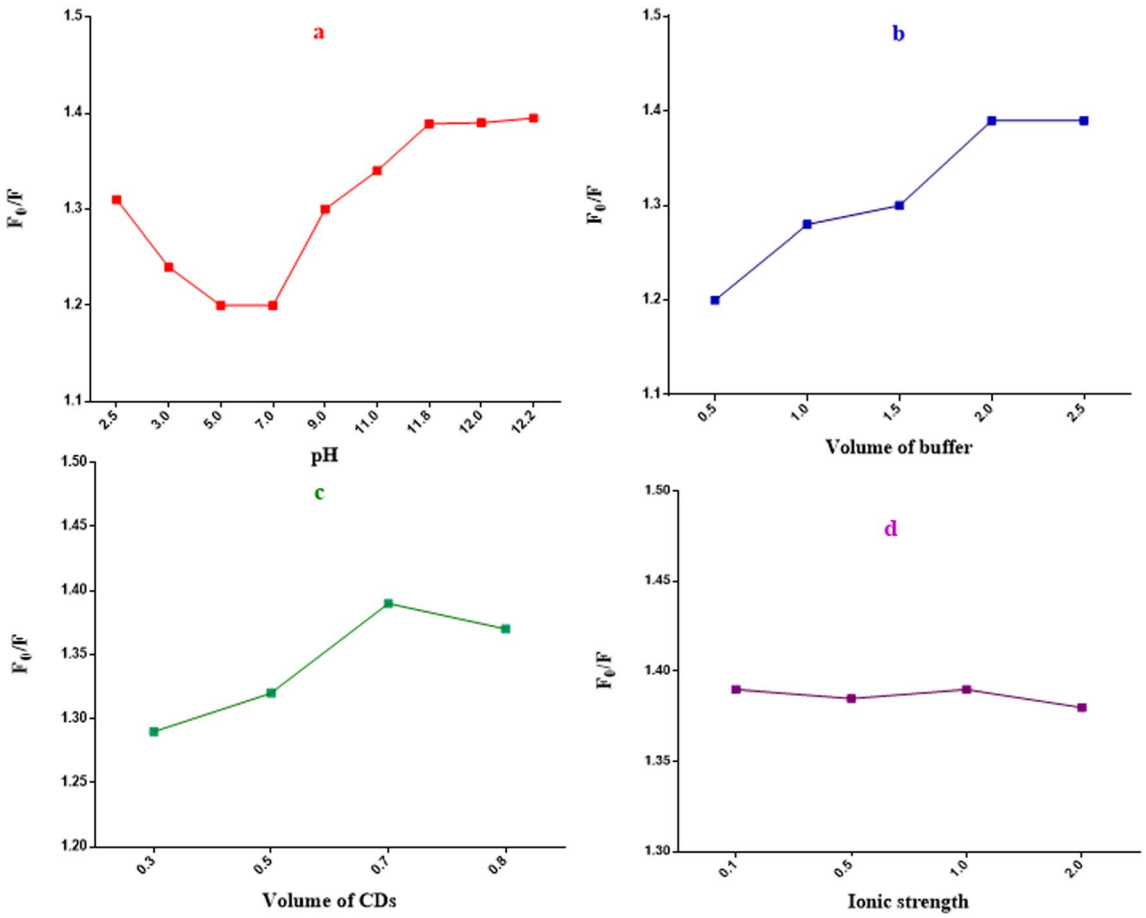

Fig. 6 Influences of different experimental parameters in the quenching efficiency of N,S-CDs: (a) pH of the buffer solution, (b) buffer volume, (c) N,S-CDs volume and (d) ionic strength.

Table 1 Analytical performance data for the spectrofluorometric determination of BTM using the fluorescence sensor[a]

Parameter	Range/value
Concentration range (μM)	1.0–100.0
Correlation coefficient	0.9999
Intercept ± S_a	$-0.02 \pm 17 \times 10^{-4}$
Slope ± S_b	$0.17 \pm 3 \times 10^{-4}$
Detection limit	0.33
Quantification limit	0.99
$S_{y/x}$	28×10^{-4}
RSD (%)	1.13
Er (%)	0.43

[a] S_a: symbol for standard deviation of intercept, S_b symbol for standard deviation of slope, $S_{y/x}$: symbol for standard deviation of residuals, RSD: symbol for a relative standard deviation, while Er: symbol for error.

$$\ln F_0/F = 0.17C - 0.02 \ (r = 0.9999).$$

where F_0 and F are the relative fluorescence intensities for the reagent blank and the drug, respectively, C is the concentration of BTM (μm) and r is the correlation coefficient.

The sensitivity of the method was demonstrated by low values of limits of detection and quantification (LOD and LOQ). The LOD and LOQ values were 0.33 μM and 0.99 μM, respectively as abridged in (Table 1).

To ensure the accuracy of the method, the output data from the proposed method was compared with those given by a reported HPLC method.[4] Upon statistical analysis of the data, it was found that there was no significant difference according to Student's t-test and variance ratio F-test[33] as shown in (Table 2).

The precision of the method was inquired through measuring three different concentrations of BTM in pure form in the same day and for three successive days and each concentration was measured in a triplicate manner. In virtue of the resulted data (low values of RSD% < 2), the method possessed high reproducibility and repeatability as shown in (Table 3).

The robustness of the proposed method was furthermore confirmed, as there was no significant effect on the analytical results or the percent recoveries upon performing minor changes in pH (12 ± 0.2) or in buffer volume (2.0 ± 0.2 mL) as shown in (Table S1†).

Table 3 Precision data from the spectrofluorometric assay of BTM *via* using the fluorescence sensor

		BTM concentration (μM)		
Parameters		10.0	30.0	50.0
Intra-day	Recovery[a] (%)	97.16	99.72	100.22
		98.54	99.32	98.52
		97.77	100.21	99.96
	$\bar{X}$	97.82	99.75	99.57
		99.55		
	±SD	0.7	0.45	0.92
	RSD (%)	0.70	0.45	0.92
	Error (%)	0.41	0.26	0.53
Inter-day	Recovery[a] (%)	97.16	99.72	100.22
		100.29	99.63	101.46
		98.07	101.09	98.21
	$\bar{X}$	98.51	100.15	99.96
	±SD	1.60	0.82	1.64
	RSD (%)	1.60	0.82	1.65
	Error (%)	0.94	0.47	0.95

[a] The mean recovery of three individual determinations.

Specificity of the method means its capability to detect BTM among complex matrix of plasma or various excipients such as magnesium stearate, avisil and dextrose which are incorporated into the capsule dosage form. This method showed good specificity as no interference from any adjuvants was noticed in the assay of BTM in dosage form or in spiked plasma and high percent recoveries and low value of SD were found (Table 4).

Also, selectivity of the method was investigated through the addition of different inactive species that could exist in the BTM's matrix during its analytical determination such as, Na^+, K^+, Mg^{2+}, NH_4^+, Zn^{2+}, Cl^-, SO_4^{2-}, sodium dihydrogen orthophosphate hydrate, oxalic acid, lactose, glucose and starch. As appeared in (Fig. 7), in case of absence or presence of such materials, there is no obvious interference. In addition, investigation of the tolerance limits of the co-administered drugs

Table 2 Comparison between the percent recoveries of BTM in pure form using the proposed method and a reported one

Proposed method			Reported method[4]
Amount taken (μM)	Amount found (μM)	Recovery[a] (%)	Recovery[a] (%)
1.0	1.01	101.0	99.70
10.0	9.77	97.70	102.90
20.0	20.22	99.89	98.24
30.0	29.95	101.10	100.32
50.0	50.10	100.20	
75.0	75.11	100.15	
100.0	99.89	99.89	
$\bar{X}$ ± SD = 99.98 ± 1.13			100.29 ± 1.94
t-Test = 0.34 (2.26)[b]			
F-Value = 2.99 (8.94)[b]			

[a] The mean recovery of three separate determinations. [b] Figures between brackets are the tabulated t and F-values at ($P = 0.05$).[33]

Table 4 Comparison between the percent recoveries of BTM in-lab prepared capsules and in spiked human plasm thorough the proposed spectrofluorometric method and the comparison HPLC one

	Proposed method			Comparison method[4]
Drug (BTM)	Amount taken (μM)	Amount found (μM)	Recovery[a] (%)	Recovery[a] (%)
In-lab prepared BTM capsules	20.0	20.28	101.42	98.00
	40.0	41.14	102.84	98.65
	60.0	61.82	103.03	101.33
$\bar{X} \pm$ SD	102.43 ± 0.88			99.33 ± 1.77
t-Test	2.26 (2.78)[b]			
F-Value	4.03 (19.0)[b]			
Spiked human plasma	1.0	0.98	98.03	97.22
	1.6	1.60	99.87	98.00
	2.0	2.02	100.73	102.05
	2.4	2.48	103.31	
	3.0	2.95	98.40	
$\bar{X} \pm$ SD	100.07 ± 2.12			99.09 ± 2.59
t-Test	0.59 (2.45)[b]			
F-Value	1.5 (19.25)[b]			

[a] The average of three individual determinations. [b] Figures between brackets are the tabulated *t* and *F*-values at ($P = 0.05$).[33]

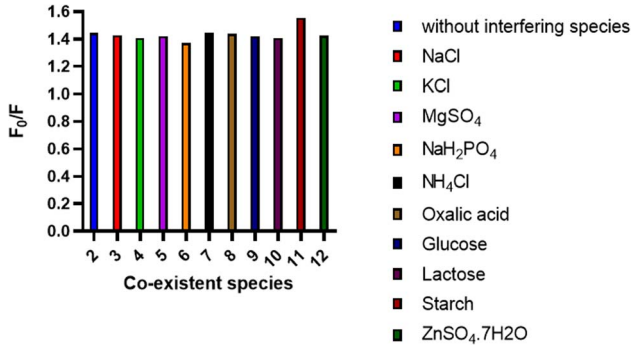

Fig. 7 Effect of some common interfering species (1.0 mM) on the spectrofluorometric determination of the BTM (20.0 μm) using the N,S-CDs sensor.

Table 5 Effect of co-administered drugs on the proposed spectrofluorometric method for determination of the BTM

Drug	Tolerance limit (μM)
Lercanidipine hydrochloride	280.0
Rosuvastatin calcium	137.0

lercanidipine HCL and rosuvastatin calcium results in high values of tolerance limits that proved the acceptable selectivity of the proposed method (Table 5).

Application

Estimation of BTM in laboratory prepared capsules. The evolved spectrofluorometric method was employed for estimation of BTM in its laboratory prepared capsules. Upon analyzing three different concentrations of BTM in-lab prepared capsules, precise results were obtained and were found to be convenient with labeled claim as illustrated by the high percent recoveries with low SD value (Table 4). Moreover, comparing these results with other HPLC reported method[4] was applied through Student's *t*-test and variance ratio *F*-test,[33] and the relevant of the results ensured the aptness of the proposed method for pharmaceutical application.

Estimation of BTM in spiked human plasma. Furthermore, the high sensitivity of the developed method assisted to estimate BTM in spiked human plasma sample. The working range of the method is 1.0–100.0 μM (0.568–56.8 μg mL^{-1}). The high dose regimen of the drug results in a therapeutic drug level of about 1.6 μg mL^{-1}, which lies within the working range of the developed method. Also, in case of toxicity of BTM or overdose for in-patient, this method can be adopted. Five different concentrations within the linear concentration range of BTM were investigated. Likewise, the *in vitro* determination of BTM was proved to be effective, specific and accurate as represented in high percentage recoveries and low percentage error values (Table 4). Furthermore, the comparison between the results evolved from the proposed method and comparison one[4] ensured the good agreement adopting Student's *t*-test and variance ratio *F*-test[33] as seen in (Table 4).

ComplexGapi approach for greenness evaluation. The philosophy of green chemistry mainly stands on the concept of conducting processes that are concurrent with basics of sustainable development. Recently, scientists exert their efforts to develop green and sustainable methods in many fields, such as in quality control laboratories, technology development and industrial management. From this context, finding the perfect tool for evaluation the green character of the proposed analytical procedure must be taken in consideration. There are different analytical tools that could evaluate the greenness such as: national environmental methods index (NEMI), advanced pictograms, analytical eco-scale, analytical GREEnness and

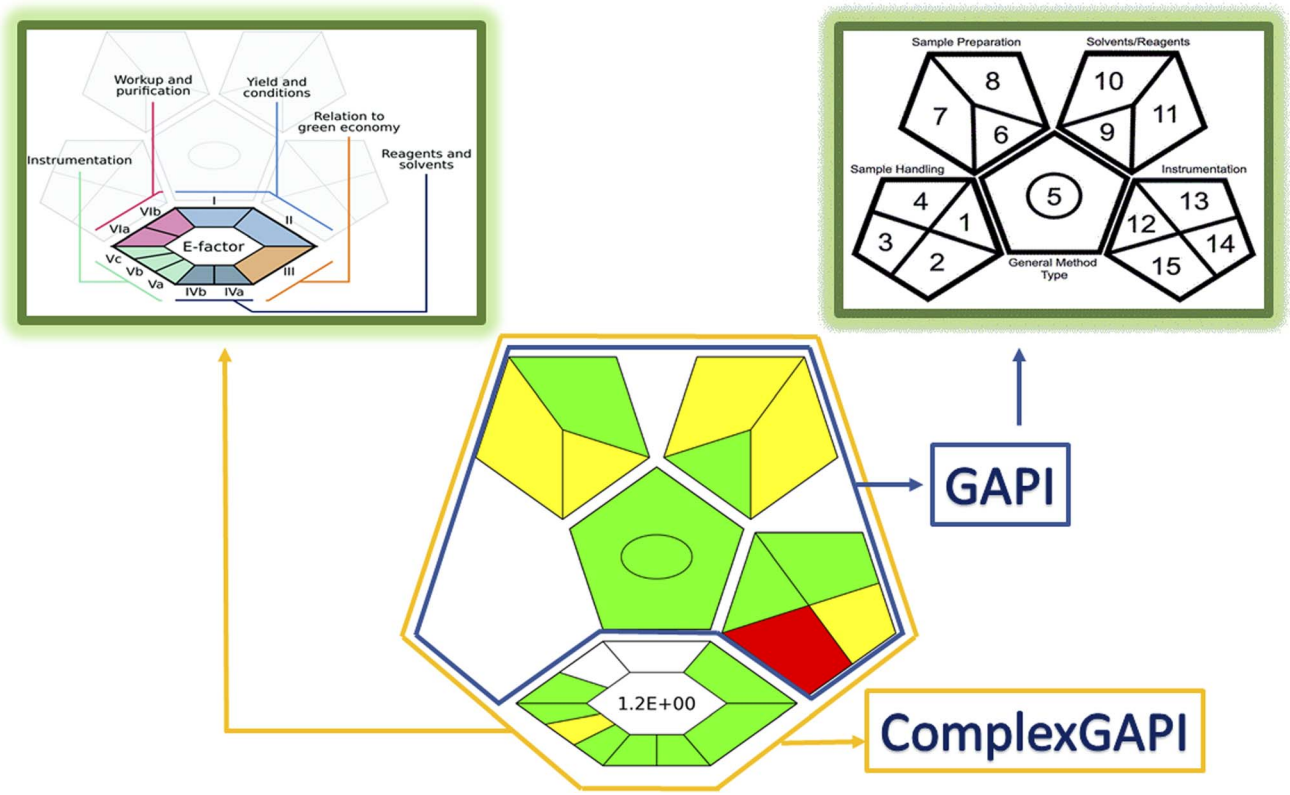

Fig. 8 ComplexGAPI approach results for greenness evaluation of the proposed method.

GAPI approaches. All these methods have different defects and drawbacks.[34] The complementary green analytical procedure index (ComplexGapi approach) is a new and comprehensive tool of greenness assessment that combines the ability to evaluate both the analytical procedure and the process which is followed to progress the analytical procedure itself.[34] Where an extra hexagonal ring was added to the GAPI pictogram to show the greenness aspect of the listing parameters such as, yield & conditions, solvents & reagents and instrument with purification. These parameters could evaluate the greenness of synthesis process of nanosensors. Different colors of pictograms are corresponding to the degree of greenness. Where, red, yellow and green colors reflect the high, medium and low environmental efficacy, respectively. The superiority of using ComplexGapi approach lies in its ability to evaluate the whole protocol in the proposed method with the availability of the software that will expand the applicability of such a solution.[34] The greenness of the process that was followed to synthesize the N,S-CDs, and the analytical procedure for quantitative determination of BTM were tested. The green profile of the performed study was proved upon using ComplexGapi approach, which encourages its application in quality control laboratories as seen in (Fig. 8).

Comparative study between the performance of the evolved method and the other reported ones for determination of BTM. Upon performing a comparative study between the proposed method and other reported ones (Table S2†), the proposed method possessed superiority and inserted many advantages. The N,S-CDs probe succeeded in determination of BTM with a better sensitivity of 2–176 times than the other reported methods.[5,7,8] There were no hazardous, harsh or expensive chemicals used in the proposed method as found in HPLC or LC/MS-MS techniques.[4–6] Despite these methods[4–6] are more sensitive than the evolved one, but the ecological aspect with integrating green chemistry in the evolved method gave it the preference. Furthermore, the synthesized N,S-CDs probe is characterized by ultra-fast determination unlike the other techniques, which are time consuming and need a long time for conditioning, washing and analysis.

Conclusion

The proposed method introduced a new optical sensor (N,S-CDs) that was evolved *via* microwave irradiation route from simple and eco-friendly precursors as sucrose (source for C) and thiourea (source for N,S) for precise estimation of BTM in bulk, in-lab prepared capsules and in spiked human plasma. The spectrofluorometric method for determination of BTM is depending on quenching the intense fluorescence that brighten from N,S-CDs. These dots possessed high water solubility, minimal toxicity, good chemical stability and biocompatibility. The preference of the sensing system is summarized in its high sensitivity, simplicity, rapidity and sustainability. ComplexGapi approach clarified the green profile of the conducted method and encouraged its applicability in pharmaceutical companies and in sustainable development projects.

Author contributions

Mariam S. El-Semary: methodology, formal analysis, investigation, validation, data curation, writing original draft. Ali A. El-Emam: validation, project administration, supervision, review and editing. F. Belal: conceptualization, resources, validation, project administration, supervision, review and editing, Amal A. El-Masry: conceptualization, methodology, formal analysis, investigation, validation, resources, data curation, writing original draft, writing-review and editing.

Conflicts of interest

The authors declare that they have no competing interests.

Acknowledgements

The authors appreciate the donation of the instrument used in this study (Cary Eclipse Spectrofluorometer) by the Alexander von Humboldt foundation to one of the authors (Prof. F. Belal).

References

1 J. E. Ansell, in *Consultative Hemostasis and Thrombosis*, ed. C. S. Kitchens, C. M. Kessler, B. A. Konkle, M. B. Streiff and D. A. Garcia, Elsevier, Philadelphia, 4th edn, 2019, pp. 747–777, DOI: 10.1016/B978-0-323-46202-0.00037-6.
2 N. C. Chan, V. Bhagirath and J. W. Eikelboom, *Vasc. Health Risk Manage.*, 2015, **11**, 343–351.
3 P. Zhang, W. Huang, L. Wang, L. Bao, Z. J. Jia, S. M. Bauer, E. A. Goldman, G. D. Probst, Y. Song, T. Su, J. Fan, Y. Wu, W. Li, J. Woolfrey, U. Sinha, P. W. Wong, S. T. Edwards, A. E. Arfsten, L. A. Clizbe, J. Kanter, A. Pandey, G. Park, A. Hutchaleelaha, J. L. Lambing, S. J. Hollenbach, R. M. Scarborough and B. Y. Zhu, *Bioorg. Med. Chem. Lett.*, 2009, **19**, 2179–2185.
4 A. A. El-Masry, D. R. El-Wasseef, M. Eid, I. A. Shehata and A. M. Zeid, *J. Chromatogr. Sci.*, 2021, **59**, 785–794.
5 P. Harshalatha, K. Chandrasekhar and M. V. Chandrasekhar, *Int. J. Res. Pharm. Sci.*, 2018, **9**, 1572–1578.
6 T. Jasemizad and L. P. Padhye, *MethodsX*, 2019, **6**, 1863–1870.
7 A. A. El-Masry, D. R. El-Wasseef, M. Eid, I. A. Shehata and A. M. Zeid, *R. Soc. Open Sci.*, 2022, **9**, 211457.
8 A. El-Masry, A. Zeid, D. El-Wasseef, M. Eid and I. Shehata, *Anal. Chem. Lett.*, 2020, **10**, 768–783.
9 X.-Y. Zhang, Y. Li, Y.-Y. Wang, X.-Y. Liu, F.-L. Jiang, Y. Liu and P. Jiang, *J. Colloid Interface Sci.*, 2022, **611**, 255–264.
10 W. Shi, F. Guo, M. Han, S. Yuan, W. Guan, H. Li, H. Huang, Y. Liu and Z. Kang, *J. Mater. Chem. B*, 2017, **5**, 3293–3299.
11 Z. Ding, F. Li, J. Wen, X. Wang and R. Sun, *Green Chem.*, 2018, **20**, 1383–1390.
12 A. Alaghmandfard, O. Sedighi, N. Tabatabaei Rezaei, A. A. Abedini, A. Malek Khachatourian, M. S. Toprak and A. Seifalian, *Mater. Sci. Eng., C*, 2021, **120**, 111756.
13 C. Lin, H. Liu, M. Guo, Y. Zhao, X. Su, P. Zhang and Y. Zhang, *Colloids Surf., A*, 2022, **646**, 128962.
14 Y. Xie, Y. Zhou, C. Gao, L. Liu, Y. Zhang, Y. Chen and Y. Shao, *Sep. Purif. Technol.*, 2022, **303**, 122288.
15 Y. Wan, M. Wang, K. Zhang, Q. Fu, M. Gao, L. Wang, Z. Xia and D. Gao, *Microchem. J.*, 2019, **148**, 385–396.
16 S. Choudhary, B. Joshi and A. Joshi, *ACS Food Sci. Technol.*, 2021, **1**, 1068–1076.
17 Y. Xue, C. Liu, G. Andrews, J. Wang and Y. Ge, *Nano Convergence*, 2022, **9**, 15.
18 Q. Geng, H. Wang, J. Wang, J. Hong, W. Sun, Y. Wu and Y. Wang, *Small Methods*, 2022, **6**, 2200314.
19 Z. Ding, X. Mei and X. Wang, *Nanoscale Adv.*, 2021, **3**, 2529–2537.
20 H. Tetsuka, A. Nagoya, T. Fukusumi and T. Matsui, *Adv. Mater.*, 2016, **28**, 4632–4638.
21 G. Magdy, A. F. Abdel Hakiem, F. Belal and A. M. Abdel-Megied, *Food Chem.*, 2021, **343**, 128539.
22 S. M. Abd Elhaleem, F. Elsebaei, S. Shalan and F. Belal, *Luminescence*, 2022, **37**, 713–721.
23 C. Würth, M. Grabolle, J. Pauli, M. Spieles and U. Resch-Genger, *Nat. Protoc.*, 2013, **8**, 1535–1550.
24 H. T. S. Britton and R. A. Robinson, *J. Chem. Soc.*, 1931, 1456–1462, DOI: 10.1039/JR9310001456.
25 Z. Lou, H. Huang, M. Li, T. Shang and C. Chen, *Materials*, 2013, **7**, 97–105.
26 A. Nandiyanto, R. Oktiani and R. Ragadhita, *Indones. J. Sci. Technol.*, 2019, **4**, 97–118.
27 P. Devi, S. Saini and K.-H. Kim, *Biosens. Bioelectron.*, 2019, **141**, 111158.
28 P. Anilkumar, X. Wang, L. Cao, S. Sahu, J.-H. Liu, P. Wang, K. Korch, K. N. Tackett II, A. Parenzan and Y.-P. Sun, *Nanoscale*, 2011, **3**, 2023–2027.
29 S. Miao, K. Liang, J. Zhu, B. Yang, D. Zhao and B. Kong, *Nano Today*, 2020, **33**, 100879.
30 F. Zu, F. Yan, Z. Bai, J. Xu, Y. Wang, Y. Huang and X. Zhou, *Microchim. Acta*, 2017, **184**, 1899–1914.
31 R. El-Shaheny, S. Yoshida and T. Fuchigami, *Microchem. J.*, 2020, **158**, 105241.
32 ICH Harmonized Tripartite Guideline, *Validation of Analytical Procedures: Text and Methodology, Q2(R1), Current Step 4 Version, Parent Guidelines on Methodology Dated November 6 1996*, Incorporated in November 2005, http://www.ich.org/products/guidelines/quality/article/quality-guidelines.html, accessed May 18th, 2017.
33 J. C. M. and J. N. Miller, *Statistics and Chemometrics for Analytical Chemistry*, Pearson Education Limited, Harlow, England, 6th edn, 2010.
34 J. Płotka-Wasylka and W. Wojnowski, *Green Chem.*, 2021, **23**, 8657–8665.